Arch. Metall. Mater. **68** (2023), 3, 955-960

DOI: https://doi.org/10.24425/amm.2023.145459

D.-P. BURDUHOS-NERGIS[1], C. BEJINARIU[1], A.M. CAZAC[1], A.V. SANDU[1], P. VIZUREANU[1*]

XRD AND STA CHARACTERIZATION OF PHOSPHATE LAYERS DEPOSITED ON THE CARBON STEEL SURFACE

Carbon steel is one of the most widely used alloys in many industries, however, its use is limited by its low corrosion resistance. Depositing a layer of phosphate on its surface improves the corrosion resistance as well as other properties, such as wear resistance, adhesion etc. Accordingly, preliminary studies demonstrated that carbon steel coated with phosphate layers can be used in the manufacture of carabiners for various fields: civil engineering, oil industry etc. Whereas, to demonstrate their capacity to operate in severe conditions related to fire rescue and extinguishing operations, it is necessary to evaluate the thermal behaviour of these materials. Thus, the main goal of this paper is to study the behaviour at high temperatures of three different types of phosphate layers deposited on carbon steel surface, by STA analysis. Also, the paper aims to study the formation of different phosphate layers by determining the types of compounds formed after the completion of the phosphating process, by XRD analysis.

Keyword: Zinc phosphate; Manganese phosphate; carbon steel; XRD; STA

1. Introduction

The personal protective equipment used by firefighters in rescue/evacuation operations during firefighting contains parts made of carbon steel, due to the good mechanical properties and the low manufacturing cost. These components can be of the type of hooks or carabiners and have the role of keeping the elements of the system together [1].

There are a multitude of standards that recommend the removal of these components when oxides are formed on their surface, which lead to a decrease in the mechanical properties of the material, respectively the protection assembly [2-6].

It is well known that carbon steel has superior mechanical properties [7], but like any other material, it also has weak points. In the case of carbon steel, the low corrosion resistance is the main reason why much personal protective equipment is withdrawn from use [8,9].

Several studies [10-13] have been carried out to improve the corrosion resistance of carbon steel in different environments, without significantly increasing its manufacturing cost. This was possible by depositing a layer of phosphate on the surface of the carbon steel by conversion.

The process by which the layer was deposited is called phosphating and is one of the most used deposition methods to improve the corrosion resistance and wear of metallic materials [14,15]. This process is used in a variety of areas such as civil construction [16], automotive industry [17], plastic deformation processing [18] etc.

The paper studies the formation of three different phosphate layers by determining the compounds formed on the surface of carbon steel following the phosphating process, by X-Ray Diffraction analysis (XRD). Also, to conclude whether the carbon steel connectors coated with a phosphate layer can be used by firefighters in rescue/evacuation operations during a fire, the high-temperature behaviour of three types of phosphate layers was analyzed, by Simultaneous Thermal Analysis (STA).

2. Experiment

The base material used is C45 carbon steel, with the chemical composition presented in previous studies [19]. The phosphate layer was immersed for 30 minutes in the phosphating solutions. For the phosphate layer to deposit uniformly on the entire surface of the steel, before phosphating the samples were prepared by immersion in a degreasing solution and subsequently in a pickling solution [20]. For the actual phosphating of the samples, three different phosphating solutions were used. The

[1] "GHEORGHE ASACHI" TECHNICAL UNIVERSITY OF IASI, FACULTY OF MATERIALS SCIENCE AND ENGINEERING, 41 "D. MANGERON" STREET, 700050, IASI, ROMANIA

* Corresponding author: peviz2002@yahoo.com

only difference between the three solutions, in terms of chemical composition, is the metal ions dissolved in phosphoric acid (zinc, zinc/iron and manganese). The samples obtained by immersion in the zinc-based solution were symbolized with I-Zn, those with zinc / iron-II-Zn / Fe and those with manganese III-Mn.

Structural characterization by X-ray diffraction (XRD) was performed to highlight the main types of crystals that form the phosphate coat deposited on the surface of carbon steel, as well as to confirm the composition of the deposited coats (Zayed et al., 2009). To determine the types of crystals existing on the surface of carbon steel following its phosphating with three different solutions, $10\times10\times3$ mm^3 samples were used. Crystallographic characterization of phosphate coats was done using the Panatical X'Pert Pro MPD equipment equipped with a single channel detector and a copper X-ray tube. This study used a θ-2θ angle range between 5°÷90°, the number of steps: 6093, step size: 0.0131303° every 60 seconds with a scanning speed of 0.054710°/s. To obtain the diffractograms of the phosphate coats, the collected data were processed with the Highscore Plus program version 4.8.

The thermal stability of phosphate coats deposited by conversion on the surface of carbon steel samples was determined using simultaneous thermal analysis equipment, model LINSEIS STA PT-1600 equipped with LINSEIS L81PT software. To perform this determination using differential thermal analysis (DTA) and thermogravimetry analysis (TGA), the samples were cut to specific dimensions of the crucible, so that their mass is less than 50 mg. After cutting, the samples underwent phosphating for each solution. After phosphating, the samples were weighed, their mass ranging from 45 to 50 mg. The temperature range used to determine the thermal behaviour of the coats ranged from ambient temperature (20 ± 2°C) and 600°C. The crystalline structure of hopeite, phosphophyllite and hureaulite is hydrated. Therefore, once they are subjected to a higher temperature, coat dehydration phenomena occur.

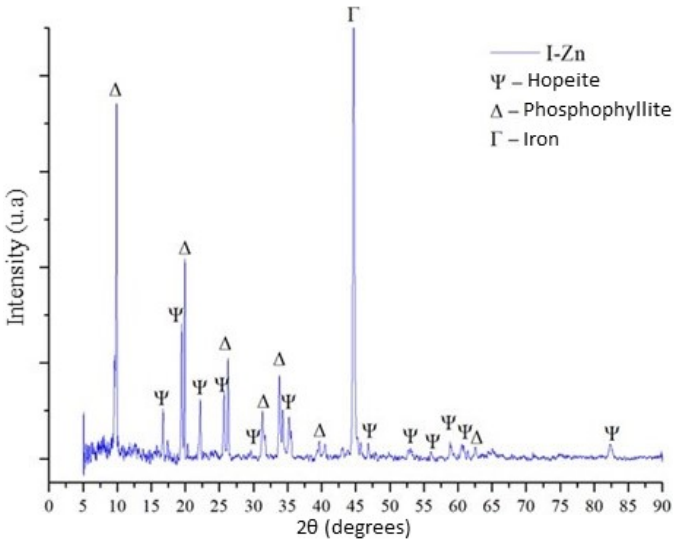

Fig. 1. Diffractogram of sample I-Zn

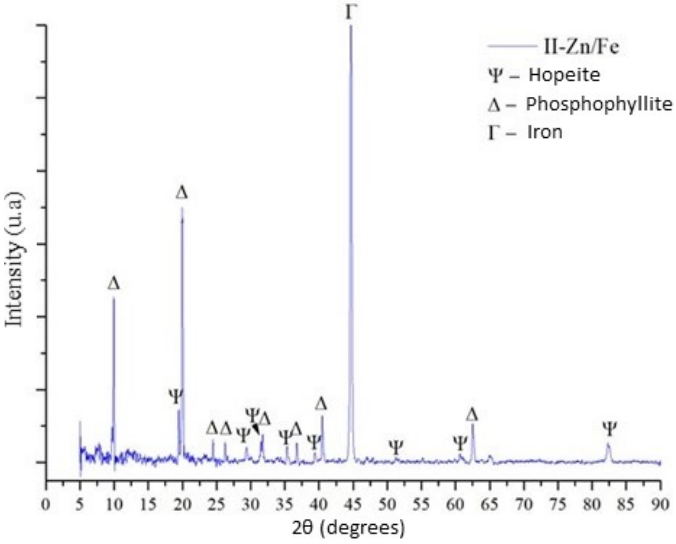

Fig. 2. Diffractogram of sample II-Zn/Fe

3. Results and Discussion

Structural characterization of phosphate coats by *X-ray diffraction*

The resulting diffractograms for the two zinc-based and zinc/iron-based coatings are shown in Figs. 1 and 2.

The XRD studies showed that phosphophyllite ($Zn_2Fe(PO_4)_2\cdot4H_2O$) and hopeite ($Zn_3(PO_4)_2\cdot4H_2O$) are the main constituents of the zinc phosphate coating of ferrous materials [17].

The mechanism of formation of zinc phosphate coats on the surface of ferrous alloys consists of three stages. In the first stage, the reversible reaction between zinc phosphate and phosphoric acid occurs, according to the reaction (Eq. (1)), resulting in zinc phosphate and free phosphoric acid.

$$3Zn\left(H_2PO_4\right)_2 \Leftrightarrow Zn_3\left(PO_4\right)_2 + H_3PO_4 \qquad (1)$$

In the next step, a hydrogen release reaction takes place in which phosphoric acid attacks the surface of carbon steel according to the reaction (Eq. (2)), resulting in ferrous dihydrogen phosphate and hydrogen.

$$Fe + 2H_3PO_4 \Leftrightarrow Fe\left(H_2PO_4\right)_2 + H_2\uparrow \qquad (2)$$

This reaction is followed by the formation of the first crystalline coat, iron phosphate, which helps to grow and form the crystalline phosphate coating. After the hydrogen is released from the solution, in the third stage, an insoluble coat of zinc phosphate (hopeite) is precipitated on the steel surface, according to the reaction (Eq. (3)).

$$\begin{array}{c} Fe + 3Zn\left(H_3PO_4\right)_2 \rightarrow F_e\left(H_2PO_4\right) + 2H_3PO_4 + H_2\uparrow \\ \downarrow \\ Zn_3\left(PO_4\right)_2\cdot4H_2O\downarrow \end{array} \qquad (3)$$

However, the reaction between the compounds present in the solution also results in the precipitation of another crystalline zinc phosphate compound (phosphophyllite), according to the reaction (Eq. (4)).

$$2Zn\left(H_2PO_4\right)_2 + Fe\left(H_2PO_4\right) + \\ + 4H_2O \rightarrow Zn_2Fe\left(PO_4\right)_2 \cdot 4H_2O \downarrow + 4H_3PO_4 \qquad (4)$$

Literature [18] has shown that the phosphophyllite on the surface of carbon steel, which crystallizes in the monoclinic crystalline system, begins to form before the hopeite that crystallizes in the orthorhombic crystalline system.

TABLE 1 illustrates the results obtained by X-ray diffraction, namely the interplanar distance and relative intensities compared to the data in the JCPDS database.

TABLE 1

XRD results for zinc phosphate coatings

		Relative Intensity [%]				
		Samples		JCPDS Data Base		
2θ	d_A [Å]	I – Zn	II – Zn/Fe	Hopeite	Phospho-phyllite	Steel
9.93	8.90	90.00	45.94		85	
19.45	4.45	38.99	80.00	40		
19.47	4.56		15.61		20	
19.99	4.46	55.02	59.39	25	100	
24.50	3.63		6.68		10	
26.27	3.39	23.72	4.05	45	60	
31.29	2.86	11.58	3.1	100	50	
31.75	2.82	18.51	5.63	15	45	
35.32	2.54		3.26	20	15	
36.74	2.45		3.26		10	
39.38	2.29	3.74	1.99	15	4	
40.46	2.23	3.26	9.00		30	
44.65	2.03	100.00	100.00			100.00
51.40	1.78		0.55	3		
60.58	1.53	3.46	1.16	13	10	
62.51	1.49	2.73	7.80		30	
82.30	1.17	3.55	3.94	70		

As one may notice both in the diffractograms shown in Figs 1 and 2 and in TABLE 1, the use of iron in the second phosphating solution leads to an increase in the phosphophyllite content deposited on the surface of the samples.

The diffractogram of the phosphate coated sample resulting from the immersion of carbon steel in the third phosphating solution is shown in Fig. 3.

The coating mechanism of sample III-Mn is different from the one of samples I-Zn and II-Zn/Fe. In this case, the first stage sees the dissociation of acid H_3PO_4 in $H_2PO_4^-$ ions, according to the reaction presented in Eq. (5) and Eq. (6).

$$H_3PO_4 \rightarrow H_2PO_4^- + H_2^+ \uparrow \qquad (5)$$

$$3Mn_2 + 2H_2PO_4 \rightarrow Mn_3\left(PO_4\right)_2 + 4H^+ \uparrow \qquad (6)$$

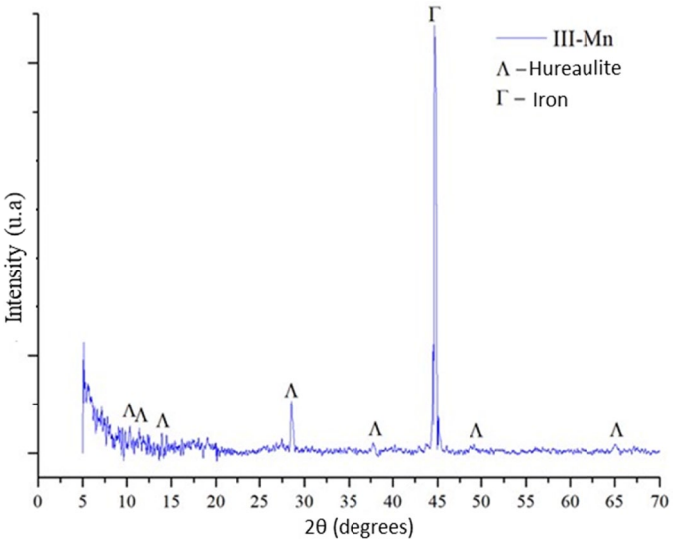

Fig. 3. Diffractogram of sample III-Mn

The second stage sees the formation of ferric phosphate resulting from the reaction Eq. (7) between iron cations and phosphate anions; this ends with the formation of the manganese phosphate precipitate on the surface of carbon steel according to reaction Eq. (8) and Eq. (9).

$$Fe_2 + PO_4^{3-} \rightarrow FePO_4 \uparrow \qquad (7)$$

$$3Mn^{2+} + 2H_2PO_4 \rightarrow Mn_3\left(PO_4\right)_2 \downarrow + 4H^+ \uparrow \qquad (8)$$

$$5Mn^{2+} + 2H_2PO_4^- \rightarrow Mn_2H_2\left(PO_4\right)_4 \downarrow + 6H^+ \uparrow \qquad (9)$$

The presence of iron in the phosphating solution determines the formation of an orthophosphate coat that crystallizes in a monoclinic crystalline system that is made of hureaulite crystals $(Mn,Fe)_5H_2(PO_4)_2 \cdot 4H_2O$ [19], as shown by Fig. 3.

Evaluation of the thermal behaviour of phosphate coats by *Simultaneous Thermal Analysis* (STA)

The thermal behaviour of the zinc phosphate and manganese coats deposited on the surface of carbon steel was determined by simultaneous thermal analysis (STA) that carries out measurements of heat flow and mass loss under the same temperature conditions.

The thermogram of the zinc phosphate coated sample, I-Zn, obtained further to DTA and TGA tests, is shown in Fig. 4.

The thermogram of the zinc phosphate coat has a specific mass loss curve (TG), which highlights the decrease of the sample mass over the entire temperature range analyzed. Water is the main compound to which weight loss is due. The curve shows a greater slope in the 20÷300°C range due to the loss of free water on the sample surface up to about 150°C and continues with water loss through the pores of the phosphate coat. When the temperature approaches 300°C, the dehydration of the

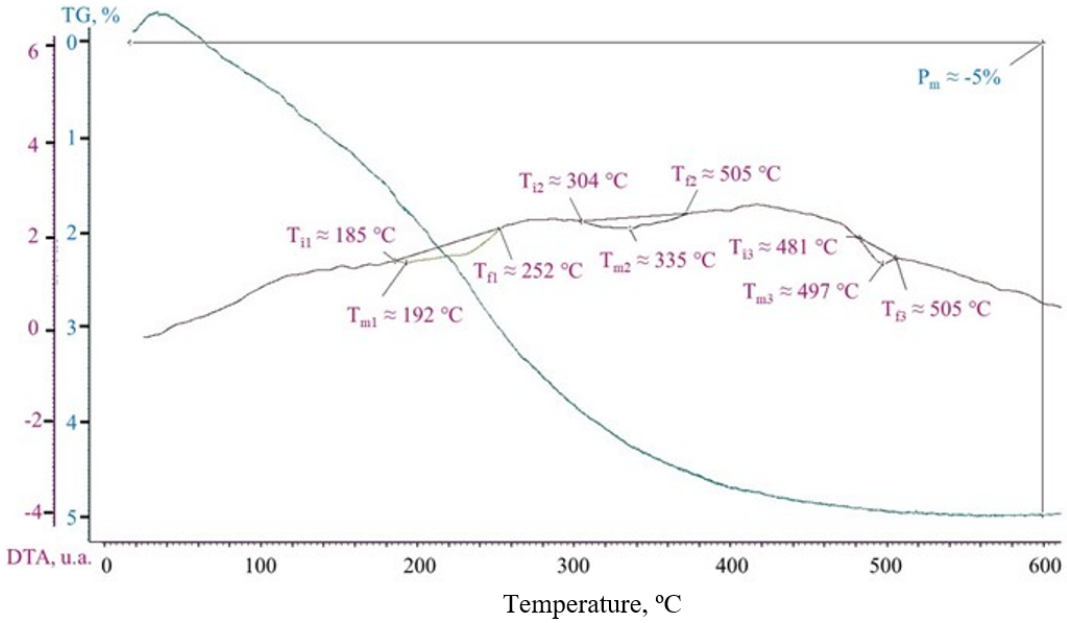

Fig. 4. The thermogram obtained for the I-Zn sample

phosphate coat begins by hopeite decomposition, a compound confirmed by the XRD results.

The DTA curve shows several inflexion points spread over large temperature ranges, which are due to the overlapping of hopeite dehydration, water evaporation or water condensation reactions.

However, the DTA curve of the sample shows an inflexion point specific to an endothermic reaction starting at an initial 481ºC temperature (T_{i3}) and ending at about 505°C (T_{f3}), the lowest temperature (T_{m3}) being 497°C. Its negative value proves the endothermic nature of the reaction, which represents the decomposition of the phosphate coat.

The zinc phosphate coated sample loses 5% of its mass within the 20°C÷600°C temperature range (P).

After changing the concentrations of the substances in the first phosphating solution and adding iron, the thermogram of sample II-Zn/Fe is shown in Fig. 5.

In this case, the mass loss in the analyzed temperature range increased from 5% to 6%, this may be due to the higher amount of free water in the structure of the phosphate coat.

The endothermic reaction occurs at the initial 483°C temperature (T_{i3}) and ends at 504°C (T_{f3}), showing an inflexion point on the DTA curve.

However, the thermal behaviour of the two samples is similar, since the ratio between the amount of phosphophyllite and hopeite is very small, according to the XRD findings. The thermogram of the manganese phosphate coated sample recorded from the DTA and TGA tests is shown in Fig. 6.

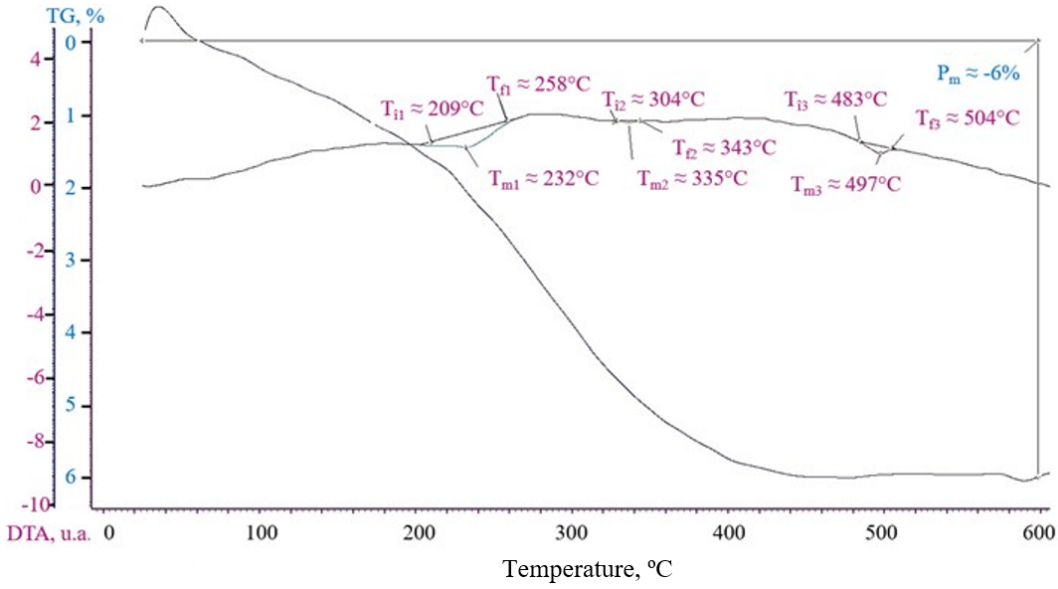

Fig. 5. The thermogram obtained for the II-Zn/Fe sample

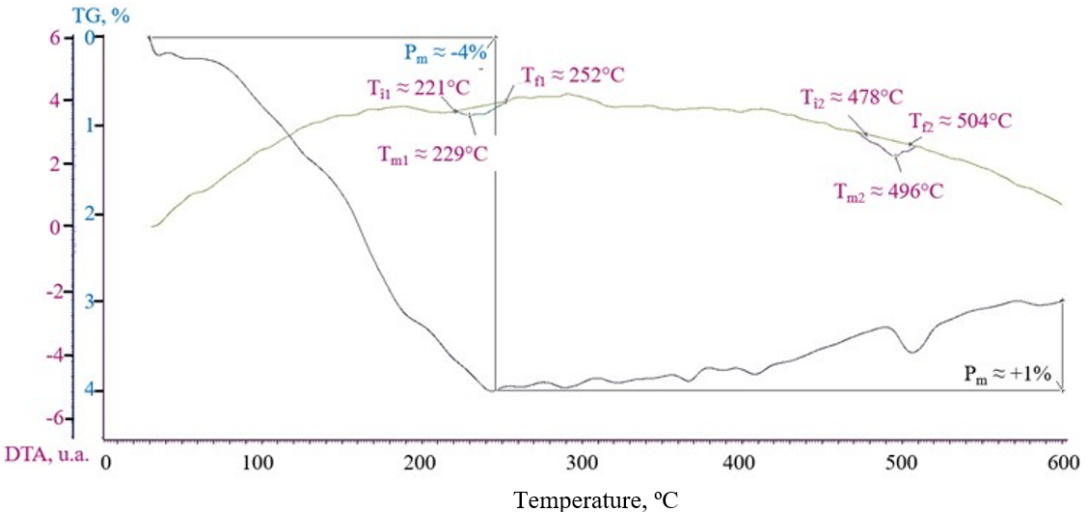

Fig. 6. The thermogram obtained for the III-Mn sample

As the porosity of manganese coats is higher than that of zinc coats, the amount of free water on the surface and in the pores is much higher, this being confirmed by the FTIR findings, where vibrations occur in the vibration band ranging between 1700 and 1500 cm^{-1} due to the H-O-H groups. Therefore, the TG curve shows a sharp decrease to about 240°C, which is due to the 4% mass decrease. Above this temperature, the curve has several inflexion points that correspond to the overlapping hureaulite oxidation and dehydration reactions.

The linear instability of the curve is due to the fact that immediately after dehydration of the compounds in the coat the substrate is exposed and it oxidizes rapidly. Therefore, the mass increase is due to oxidation, and the decrease is specific to coat dehydration.

The endothermic reaction specific to the destruction of the phosphate coat begins at an initial temperature of 478°C and ends at a temperature of 504°C.

From the point of view of thermal behaviour, the samples show coat destruction reactions within the 478÷505°C temperature range. Above this temperature, the corrosion resistance of the samples decreases.

4. Conclusions

The I-Zn, II-Zn/Fe and III-Mn sample diffractograms reveal the presence of compounds (hopeite, phosphophyllite and hureaulite) specific to each type of solution, which was formed on the carbon steel surface. The phosphophyllite concentration increases once iron is introduced in the phosphating solution II-Zn/Fe.

As far as thermal behaviour is concerned, the samples show coat destruction reactions within the 478-505°C temperature range, which means that carbon steel carabiners on which a coat of phosphate has been deposited can be used without suffering any changes, at the rescue/evacuation operations by firefighters during fires. Above this temperature, the corrosion resistance of the samples decreases.

Therefore, the phosphate coating represents an alternative method to protect de carbon steel carabiners, used by firefighters, against corrosion.

REFERENCES

[1] V. Scott, MEng, Design of a Composite Carabiner for Rock Climbing, Imperial College London, London, United Kingdom (2008).

[2] C.M. Bright, MEng Honors Theses, A History of Rock Climbing Gear Technology and Standards, University of Arkansas, Fayetteville, USA (2014).

[3] British Standards Institution, BS EN 360:2002, Personal Protective Equipment against Falls from a Height – Retractable Type Fall Arresters (2002).

[4] British Standards Institution, BS EN 365:2004, Personal Protective Equipment against Falls from a Height: General Requirements for Instructions for Use, Maintenance, Periodic Examination, Repair, Marking and Packaging (2004).

[5] British Standards Institute, BS EN 12275:2013, Mountaineering equipment. Connectors. Safety requirements and test methods (2013).

[6] British Standards Institute, BS EN 363:2008, Personal Fall Protection Equipment – Personal Fall Protection Systems (2008).

[7] D.P. Burduhos-Nergis, C. Baciu, P. Vizureanu, N.M. Lohan, C. Bejinariu, Materials Types and Selection for Carabiners Manufacturing: A Review, in Proceedings of the IOP Conference Series: Materials Science and Engineering, Institute of Physics Publishing, **572**, (2019.

[8] D.P. Burduhos-Nergis, C. Nejneru, D.C. Achiţei, N. Cimpoieşu, C. Bejinariu, Structural Analysis of Carabiners Materials Used at Personal Protective Equipments, in Proceedings of the IOP Conference Series: Materials Science and Engineering; Institute of Physics Publishing, **374** (2018).

[9] C. Bejinariu, D.P. Burduhos-Nergiș, N. Cimpoeșu, M.A. Bernevig-Sava, S.L. Toma, D.C. Darabont, C. Baciu, Quality – Access to Success. **20**, 71-76 (2019).

[10] D.P. Burduhos Nergis, C. Nejneru, D.D. Burduhos Nergis, C. Savin, A.V. Sandu, S.L. Toma, C. Bejinariu, Revista de Chimie **70**, 215-219 (2019).

[11] C. Bejinariu, D.-P. Burduhos-Nergis, N. Cimpoesu, Materials **14** (1), 188 (2021).

[12] D.-P. Burduhos-Nergis, P. Vizureanu, A.V. Sandu, C. Bejinariu, Materials **13** (15), 3410 (2020).

[13] M. Manna, Surface and Coatings Technology **203**, 1913-1918 (2009).

[14] B. Díaz, L. Freire, M. Mojío, X.R. Nóvoa, Journal of Electroanalytical Chemistry **737**, 174-183 (2015).

[15] D.P. Burduhos-Nergis, P. Vizureanu, A.V. Sandu, C. Bejinariu, Applied Sciences **10** (8), 2753 (2020).

[16] D.-P. Burduhos-Nergis, C. Bejinariu, S.-L. Toma, A.-C. Tugui, E.-R. Baciu, Carbon Steel Carabiners Improvements for Use in Potentially Explosive Atmospheres, in MATEC Web of Conferences **305**, 00015 (2020).

[17] M. Tamilselvi, P. Kamaraj, M. Arthanareeswari, S. Devikala, J. Arockia Selvi, IJACSA **3** (1), 25-41 (2015).

[18] R. Colas, G.E. Totten (Ed.), Encyclopedia of Iron, Steel, and Their Alloys, Five-Volume Set, CRC Press, Boca Raton, Florida, USA (2016).

[19] J. Duszczyk, K. Siuzdak, T. Klimczuk, J. Strychalska-Nowak, A. Zaleska-Medynska, Materials **11** (12), 2585 (2018).